Science Advances
AAAS

Supplementary Materials for

Estimating global biomass and biogeochemical cycling of marine fish with and without fishing

Daniele Bianchi*, David A. Carozza, Eric D. Galbraith, Jérôme Guiet, Timothy DeVries,

*Corresponding author. Email: dbianchi@atmos.ucla.edu

Published 8 October 2021, *Sci. Adv.* **7**, eabd7554 (2021)
DOI: 10.1126/sciadv.abd7554

The PDF file includes:

Other Supplementary Material for this manuscript includes the following:

1. Scaling model-based fish biomass estimates to a common size range

The biomass estimates summarized in Fig. 1 and Supplementary Table 1 report biomass for different consumer size classes. To facilitate a comparison, we rescale the original values to provide an approximate estimate of the biomass within a common size range appropriate for marine fish and other animals, 1g to 1000kg. To this end, we assume that the consumer size spectrum can be described by a power-law distribution, in agreement with theoretical (*64*) and observational evidence (*65*). Accordingly, the fish size spectrum can be represented as:

$f(m) = f_0 m^{-\varepsilon}$

Where f(m) is the biomass of consumers of mass m, f_0 is the spectrum intercept, and ε the exponent of the power law.

We estimate the biomass between size classes m_1 and m_2 (the original range) by integration as:

$$F(m_1, m_2) = \frac{f_0}{1-\varepsilon}({m_2}^{1-\varepsilon} - {m_1}^{1-\varepsilon}) \quad (1)$$

and the biomass between size classes m_3 and m_4 (the new range) as:

$$F(m_3, m_4) = \frac{f_0}{1-\varepsilon}({m_4}^{1-\varepsilon} - {m_3}^{1-\varepsilon}) \quad (2)$$

We can rearrange equations (1) and (2) to express the biomass in the new range as a function of the biomass in the original range, the size limits, and the exponent of the power-law, all of which are known:

$$F(m_3, m_4) = F(m_1, m_2) \cdot \frac{{m_4}^{1-\varepsilon} - {m_3}^{1-\varepsilon}}{{m_2}^{1-\varepsilon} - {m_1}^{1-\varepsilon}} \quad (3)$$

Note that in the special case of an exponent $\varepsilon = 1$ the equation above is ill-posed, but can be rewritten in the form:

$$F(m_3, m_4) = F(m_1, m_2) \cdot \frac{ln\frac{m_4}{m_3}}{ln\frac{m_2}{m_1}} \quad (4)$$

For the rescaled estimates in Supplementary Table 1, we adopt the new range from our model, that is $m_3 = 10g$ and $m_4 = 100kg$, and a constant power-law exponent of $\varepsilon = 1.05$, in line with observations (*66*), and close to the commonly adopted $\varepsilon = 1.0$ exponent of the "Sheldon spectrum" suggested in the early literature (*67*). Note that the results are not strongly sensitive to exponents in the range $\varepsilon = 1.0$ to $\varepsilon = 1.1$.

Note also that some of the original estimates in Fig. 1a consider a wider size range than 1g to 1,000kg (*20*). Hence, for these estimates the conversion to the new size range in Fig. 1b reduces the total biomass. Other estimates (including ours, labeled as "this work"), consider a smaller size

range (in our case 10g-100kg). In this case, the conversion to the new size range increases the total biomass.

2. Model formulation

2.1 Model rationale

The BiOeconomic mArine Trophic Size-spectrum (BOATS) model is organized around the mass of an individual organism, with the underlying assumption that many biological traits depend on size, including metabolic rates, life history attributes, individual interactions, and other aspects of population dynamics (*64*, *68*, *69*).

The ecological component of BOATS (Carozza, Bianchi, and Galbraith 2016) represents all potentially-targeted species with individual mass between 10 g and 100 kg, as three continuous, independent size spectra. These fish groups differ only in the asymptotic size, provide a crude representation of diversity (*70*, *71*), and are defined consistently with the sizes used in aggregated catch data (*72*). Accordingly, the asymptotic masses off small, medium, and large fish are 0.3, 8.5, and 100 kg respectively (*33*). The temporal evolution of consumer biomass follows the McKendrick-von Foerster equation (*70*, *71*), which describes processes of fish growth and mortality in size space.

Fish population dynamics such as life history, growth, mortality, reproduction and recruitment are parameterized based on relationships that draw from macroecological theory and syntheses of observational datasets. The growth rate of individual fish is equal to the photosynthetically-derived energy available to their size class via trophic transfer (*18*, *64*), divided by the number of individuals in the size class, and is capped by a temperature-dependent maximum physiological growth rate that follows well-established empirical relationships (*70*, *73*). Implicitly, the surplus of energy available to the ecosystem that is not utilized by the resolved fish spectra is assumed to be redirected to non-targeted fish groups.

Natural mortality, which includes all losses from predation, disease, parasitism and old age, but excludes fishing mortality, is a function of individual size, asymptotic size, and temperature, and follows (*74*) and (*75*). Recruitment provides the boundary condition for fish biomass spectra at their initial size, and is parameterized as a stock-recruitment relationship (*76*) that calculates the number of new recruits entering the smallest size-class as a function of primary production and the production of eggs by spawners (*70*).

The ecological model is coupled to an open-access representation of fishing effort and catch (Carozza, Bianchi, and Galbraith 2017) based on the Gordon-Schaefer fishery economics model

(*77*, *78*). Fishing catch in each size class is proportional to the fish biomass and the fishing effort through a catchability constant, and is further modulated by a size-dependent selectivity function. The catchability relates fishing catches to biomass and effort, and encapsulates the efficiency of the technology applied to fishing (*79*, *80*). Catches enter the fish equation as an additional mortality. Fishing effort evolves in time in response to catches and net revenues. The open access dynamic tends to drive the system to a state of zero net profit, where all gross revenues are dissipated to balance costs (*34*), and is a good approximation to the dynamics of fisheries under weak regulation that has characterized historical fisheries up to the period of peak catch considered here (*23*), up to the recent decades where management measures have become widespread.

2.2 Main model equations

The following is a summary of the main equations and parameters of BOATS. A complete description of the equations, and the details of the numerical implementation are provided in (*33*) and (Carozza, Bianchi and Galbraith, 2017. Supplementary Table 2 includes a list of variables and parameters entering the main equations. Supplementary Table 3 includes a list the parameter values used in the Monte Carlo and optimized ensembles, including name, symbol, units, and the parameter values expressed as mean +/- SD.

The model solves the equations for fish biomass (*f*) and fishing effort (*E*) as a function of space and time over a two-dimensional grid for the global ocean. Fish and fishing effort are divided into three groups that differ in the asymptotic size (m_∞), and are indicated with the subscript *k* in the model equations. Biomass in each group *k* is a function of the individual size *m*. We refer to the initial size of each size spectrum, m_0, as the size of recruitment. We adopt the equivalency between biomass and energy, and assume that they are related by a constant conversion factor (*81*).

The governing equation for each group biomass size spectrum (f_k) is:

$$\frac{\partial}{\partial t} f_k(m,t) = -\frac{\partial}{\partial m}\gamma_k(m,t) f_k(m,t) + \frac{\gamma_k(m,t) f_k(m,t)}{m} - [\Lambda_k(m) + q_k(t)\sigma_k(m)E_k(t)] \cdot f_k(m,t) \quad (5)$$

The first term on the right-hand side represents growth of biomass into larger size classes; the second term the increase of biomass in each size class due to individual growth, and the third term the sum of natural and fishing mortality.

The individual growth rate $\gamma_k(m,t)$ for each group at a size *m* is calculated as:

$$\gamma_k(m,t) = \left(1 - s_k(m)\frac{1-\epsilon_a}{(m/m_\infty)^{b-1}-\epsilon_a}\right) \cdot min\left(\frac{\phi_{\pi,k}\cdot\pi(m,t)\cdot m}{f_k(m,t)}, Am^b - k_a m\right) \quad (6)$$

In this equation, the second term in the first parenthesis represent the fraction of energy allocated to reproduction, and the two terms in the second parenthesis represent respectively the energy available from primary production, and the maximum potential growth rate (*73*). The energy available from primary production is calculated following (*64*) according to:

$$\pi(m,t) = \frac{\Pi_\psi(t)}{\mathrm{m}_\psi(t)}\left(\frac{m}{\mathrm{m}_\psi(t)}\right)^{\tau-1} \quad (7)$$

where $\Pi_\psi(t)$ is the vertically integrated primary production (mmolC m^{-2} s^{-1}), $m_\psi(t)$ the representative size of phytoplankton, and τ the the trophic scaling exponent, which controls how efficiently energy and biomass are transferred through the trophic web. The value of τ is calculated as $log(\alpha)/log(\beta)$ where α is the trophic efficiency and β is the predator-prey mass ratio (*64*). This equation is based on the assumption of an average predator-prey mass ratio, implying that size is equivalent to trophic level, a good assumption for heavily size-structured marine food webs (*82*). We take a single global value for the transfer efficiency, the proportion of energy available to each size class through predation that can be turned into new biomass. We assume that only a fraction $\phi_{\pi,k}$ of primary production is available to each commercial fish group. This fraction is equally partitioned among the model fish groups, such that the total fraction of primary production available to commercial fish, $\phi_\pi = \sum_k \phi_{\pi,k}$, is always between 0 and 1.

Natural mortality is a function of both individual and asymptotic size (*74*, *75*), and follows:

$$\Lambda_k(m) = \lambda m^{-h} m_{\infty,k}^{h+b-1} \quad (8)$$

The term:

$$h_k(m,t) = q_k(t)\sigma_k(m)E_k(t)f_k(m,t) \quad (9)$$

represent the catch of fish group *k* at the size *m*, and is a function of fish biomass and effort, as well as the catchability parameter *q*, a measure of the technological efficiency of fishing gear to capture fish biomass, a selectivity function $\sigma(m)$, which varies between 0 and 1 and expresses the intrinsic ability of a given gear to target a given size class *m*. In BOATS, we assume that selectivities have a sigmoidal shape, with a sharp transition at the smallest size that can be caught (*34*, *70*).

The boundary condition at the initial size class is given by the recruitment equation (*70*):

$$f_k(m_0,t)\gamma_k(m_0,t) = \frac{R_{P,k}(m_0,t)\cdot R_{e,k}(m_0,t)}{R_{P,k}(m_0,t)+R_{e,k}(m_0,t)} \quad (10)$$

where R_e is the recruitment from the survival of larvae, calculated from the product of egg production, a function of spawner biomass, and the larvae survival probability, while R_p is a potential recruitment rate, determined by the maximum energy available from primary production. All terms expressing rates, including growth and mortality rates, depend on temperature according to the van't Hoff-Arrhenius equation:

$$a(T) = exp\left[\frac{\omega_a}{k_B}\left(\frac{1}{T_r} - \frac{1}{T}\right)\right] \quad (11)$$

where (ω_a) is the activation energy, (T) the absolute temperature, (T_r) a reference temperature of 283 K, and (k_B) the Boltzmann constant. According to this formulation, for example, the allometric growth parameter is expressed as a function of temperature following:

$$A = A_0 a(T) \quad (12)$$

The governing equation for the fishing effort E_k on each group is:

$$\frac{d}{dt}E_k(t) = \kappa_e\left(q_k(t)\int_{m_0}^{m_{\infty,k}} p_k(m)\sigma_k(m)f_k(m,t)dm - c_k(t)\right) \quad (13)$$

where the first term on the right-hand side represent the catch integrated across all size classes, and the second term the cost per unit effort.

The model is solved with a forward in time, upwind in size numerical scheme, and is applied to a one-degree resolution global grid of the ocean, forced with monthly climatological temperature from the World Ocean Atlas (*83*), averaged between 0-75m, and satellite-derived primary productivity from three different algorithms (*48*).

3. Monte Carlo ensemble formulation

We perform a set of 10,000 Monte Carlo simulations in which 13 model parameters are randomly drawn from distributions estimated from the literature (*34*). These parameters (listed in Supplementary Table 3) have the largest impact on the predicted pristine biomass. Each simulation is run for 100 years with constant low catchability and negligible catches, followed by 200 years under an increase in catchability at a specific rate of 7% y^{-1}, in rough agreement with historical reconstructions that indicate values between 3 and 8% y^{-1} (*23*, *79*, *80*).

The 10,000 simulations produce pristine commercial fish biomass values over LMEs that spans 5 orders of magnitude, varying between zero to nearly 19Gt, with an average of 0.56Gt. Similarly, global peak catches range from zero to more than 1,000Mt y^{-1}. Half of the runs produce less than 16Mt y^{-1}, a gross underestimate compared to reconstructions. The low pristine biomass in the majority of the runs is hardly capable of sustaining peak catches in the range of

observations. To reduce these biases, we turn to catch reconstructions and C:B ratios from stock assessments, and select an optimized ensemble of 31 simulations that best reflect the observational constraints.

4. Constraining model catches with SAUP data, and extrapolation to the whole consumer community

In the model, a fraction $\phi_\pi = \sum_k \phi_{\pi,k}$ of the energy available to consumers from trophic transfer of primary production is made available to the resolved spectrum of commercial fish (see also equation 6). Note that the fate of the energy coming from NPP is mostly dissipation at each trophic level, since the energy available to consumers in different size classes is scaled according to equation 7). In the model runs of the optimized ensemble, we prescribe this fraction so that the global peak catch, integrated over LMEs, matches the reconstruction from the SAUP database. To this end, we calculate the global catch from the large ensemble of 10,000 simulations (where by default $\phi_\pi = 1.0$), and we reassess ϕ_π with:

$$\phi_\pi = \frac{\text{Catch(SAUP)}}{\text{Catch(model)}} \quad (14)$$

We then run two instances of the optimized ensemble of simulations with identical parameters, except for ϕ_π. In the first instance, we use variable ϕ_π based on equation 14, representing our best guess for the commercial fish fraction. In the second instance, we set $\phi_\pi = 1.0$, meaning that the model represents the entirety of the food web fueled by NPP.

The extrapolation obtained by setting $\phi_\pi = 1.0$ provides only an approximated representation of the consumer size spectrum. While the biomass of commercial fish and other consumers is calibrated against catch and biomass observations, no such observational syntheses exist at the global scale to constrain non-commercial consumers. Additionally, the model has only a limited representation of the diversity of consumers, which is tied to their asymptotic size, as commonly done in size-based models (*84*). Within each asymptotic size class, consumers are treated identically, i.e., they share physiological, life history and ecological traits. This may lead to approximations when the model is scaled up from commercial fish and other consumers to the whole animal community spectrum. As an example, the model does not distinguish between ectothermic and endothermic organisms. Because endotherms experience higher body temperatures and metabolic rates than ectotherms, the extrapolation would represent an upper boundary on consumer biomass, while providing a closer representation of consumer cycling rates, which are ultimately limited by NPP.

5. Biomass cycling rate of fish

We estimate the biomass cycled by an individual fish and returned directly to the environment $C_{i,k}(m)$ by starting from the new biomass production ξ_{net} (that is, somatic growth plus generation of reproductive material) of an individual fish in a given size class. In order to obtain the total amount of biomass that was ingested by the individual fish to generate new biomass we divide ξ_{net} by the assimilation efficiency α, to obtain the gross ingestion, and subtract from it the new biomass production ξ_{net}, so that:

$$C_{i,k}(m) = \frac{\xi_{net}}{\alpha} - \xi_{net} = \xi_{net}\frac{1-\alpha}{\alpha} \quad (15)$$

where, consistent with equation (6):

$$\xi_{net} = min\left(\frac{\phi_{\pi,k}\cdot\pi(m,t)\cdot m}{f_k(m,t)}, Am^b - k_a m\right) \quad (16)$$

Note that we subtracted the production of new biomass, because it represents biomass that remains within the size spectra, through a combination of somatic growth, predation, reproduction and recruitment. The resulting $C_{i,k}(m)$ thus provides an estimate of the biomass "processed" by each fish, and returned directly to the environment, as a combination of organic (e.g. fecal pellets, excretion) and inorganic (respiration) fluxes, but not including recycling through predation within the total fish population.

To scale up the biomass cycled by fish to the entire population, we integrate the individual metabolic demand $C_{i,k}(m)$ over the size spectrum, separately for each group *k*, and we sum over all groups, so that:

$$\mathrm{C}_{total} = \sum_k \mathrm{C}_k = \sum_k \int_{m_0}^{m_{\infty,k}} C_{i,k}(m) n_k(m) dm = \sum_k \int_{m_0}^{m_{\infty,k}} C_{i,k}(m)\frac{f_k(m,t)}{m} dm \quad (17)$$

We express C_{total} in units of wet biomass processed by fish per unit area per unit time (i.e. t km^{-2} y^{-1}). This quantity is directly comparable to the generation of new biomass from net photosynthesis, and can be expressed in units of carbon by using the conversion factors: 10g wet biomass = 1 g C = 1/12 mol C (*18*, *85*).

6. Comparison of particle export and fish-mediated export at depth

Organic particles sink and remineralize in the ocean interior producing a depth-dependent flux of organic carbon, $\Phi^p(z)$, that is well described by the widely-used power-law ("Martin curve") of the form:

$$\Phi^p(z) = \Phi_0^p\left(\frac{z}{z_e}\right)^{-b_p} \quad (18)$$

Where Φ_0^p is the particle flux leaving the euphotic zone, z_e, and b_p is the power law exponent, also known as the attenuation coefficient (*86*). The attenuation coefficient reflects the magnitude of the particle specific remineralization rate, and their sinking speed, so that faster speeds and slower rates would result in smaller attenuation coefficients (*87*).

We assume that fish-produced fecal pellets flux, $\Phi^f(z)$, follows a similar dynamic, but with a different (and presumably smaller in absolute value) attenuation coefficient b_f, and a different flux at the base of the euphotic zone, Φ_0^f:

$$\Phi^f(z) = \Phi_0^f \left(\frac{z}{z_e}\right)^{-b_f} \quad (19)$$

We compare the fish-mediated particle flux to the bulk particle flux by taking the ratio of (17) and (19):

$$\frac{\Phi^f(z)}{\Phi^p(z)} = \frac{\Phi_0^f}{\Phi_0^p}\left(\frac{z}{z_e}\right)^{b_p - b_f} \quad (20)$$

Thus, at any given depth *z*, the ratio of these two fluxes only depends on their ratios at the surface, and a function of the respective attenuation coefficients and depth:

$$\zeta_f = \left(\frac{z}{z_e}\right)^{b_p - b_f} \quad (21)$$

We compare three cases, that we label as “typical”, “weak” and “strong”. The “typical” case assumes that bulk particle fluxes remineralize with an attenuation coefficient $b_p = 0.7$, a typical ocean average (*50*), and that fish-produced particles sink at an average speed 10 times larger than bulk particles, resulting in a smaller attenuation coefficient for fish-produced particles, $b_f = 0.07$. The “weak” case assumes a that all particles remineralize at a slower rate, and sets $b_p = 0.6$ and $b_f = 0.06$. The “strong case” assumes a more rapid remineralization of bulk particles ($b_p = 0.8$), and a negligible attenuation of fish-produced particles (corresponding to sinking speed of the order of 1000m per day, the upper range of observations), obtained by setting $b_f = 0$. The results of this comparison, for a range of depths, are summarized in Supplementary Table 5.

7. Calculation of the organic particle remineralization signal from the ocean circulation inverse model

We estimate the three-dimensional distribution of the carbon released in the ocean interior by particle remineralization by solving the following equation:

$$\frac{\partial C}{\partial t} = \boldsymbol{T}C - \frac{\partial \Phi}{\partial z} \quad (22)$$

where C is the dissolved inorganic carbon (in units of $\mathrm{mmol\,m^{-3}}$) resulting from remineralization of the particulate organic carbon flux below the euphotic zone (here 74 m), Φ, and **T** is the transport operator matrix from the ocean circulation inverse model (*88*). Because C only tracks the products of remineralization, the boundary condition for C is set equal to zero at the surface. Equation 22 is solved for steady state ($\frac{\partial C}{\partial t} = 0$) by matrix inversion.

We solve two instances of equation (22). In the first instance we set the particle flux Φ equal to the flux of all sinking particles (equation 18), with a power-law exponent $b_p = 0.7$, a typical ocean average (*50*), and use particle fluxes from the euphotic zoneΦ_0, from the data-based estimate of ref. (*48*). In the second instance we set the particle flux Φ equal to the flux of fish-produced particles (equation 19), with a power-law exponent $b_f = 0.07$, mimicking the more rapid (here by a factor of 10) sinking speed of fish fecal pellets (Saba and Steinberg 2012). In this case, we set the particle flux from the euphotic zone, Φ_0, equal to the particle produced by fish, which we estimate as $\Phi_0 = 0.2 \cdot C_{total}$ where 0.2 reflect the proportion of the biomass processed by fish that is returned to the environment as fecal pellets (*49*), and C_{total} is the biomass processed by fish calculated by equation (17). For simplicity, we use the estimate of C_{total} representative of the unfished ocean (Fig. 4A). We then estimate the oxygen utilization (OU, in units of $\mathrm{mmol\,m^{-3}}$) caused by particle remineralization as OU=C*150/106, where 150:106 is a typical stoichiometric ratio for oceanic particulate organic matter (*58*).

The distribution of the OU estimated by this model is shown in Supplementary Fig. 4, where it is compared with a data-based estimate of the in situ OU, which includes a correction for the oxygen undersaturation observed in surface waters, which is propagated into the interior ocean along isopycnal surfaces (*89*). The spatial pattern of OU estimated by the model compares well with observations, but the overall magnitude of OU is smaller than observed by ~25%, with some larger biases in the upper ocean. This is expected since the export product that we use (*48*) does not include export due to migrating organisms or dissolved organic matter, which account for ~30% of global organic carbon export (*51*). Our simple particle flux formulation also neglects regional variability in particle flux attenuation due to variations in temperature, oxygen, or particle size (e.g. (*90*, *91*)) which can further influence the distribution of OU. We note that this bias does not affect our conclusions, because we focus our analysis on the effect of fish-mediated export on the component of the biological pump that we resolve, i.e. sinking particles. Indeed, analysis of different simulations with our model in which the remineralization profiles are varied, indicates that the fraction of OU caused by fish-produced particle remineralization, versus the OU produced

by all particles (Fig. 5), is robust to these biases, as long as the difference in sinking speed (the factor 10) is maintained between the two types of particles.

8. Assumptions and limitation of the work

A summary of the various assumptions and limitations of the work is presented in Supplementary Table S6.

9. Data and code

The data and code used to run the BOATS model, including parameter values for the model ensemble and forcing files is included under the Supplementary Material folder BOATS_CODE/.

Processed model output and code used to generate the paper figures is included under the Supplementary Material folder MAKE_FIGURES/.

Supplementary Table S1. Summary of model-based estimates of the biomass of fish and other consumers in the ocean, used to generate Fig. 1 in the paper. We report both the original biomass from the papers, and an estimate of the biomass for consumers between 1g and 1000kg, the range used in this study (see Note 1 and Supplementary Information Section 1).

Reference	Consumer group	Model approach	Global biomass (Gt) (as reported)	Global biomass (Gt) (sizes between 1 g to 10^6g)
(*18*)	All marine animals (10^{-5}g to 10^6g)	Global size-structured macroecological model	2.6	1.0
(*18*)	Teleost and elasmobranch fish (10^{-5}g to 10^6g)	Global size-structured macroecological model	1.0	0.4
(*14*, *18*)	Teleost fish (1g to 10^6g)	Global size-structured macroecological model	0.9	0.9
(*14*)	Teleost fish	Global food-web model (Ecopath) referenced to 1950	2.1	-
(*60*)	Teleost and elasmobranch fish	LME-scale, food-web model (Ecopath) referenced to 1950	1.1	-
(*61*)	All marine animals (trophic level > 2)	Global energy transfer model (Ecotroph) referenced to 1950	11.8	-
(*61*)	Marine predators (trophic level > 3.5)	Global energy transfer model (Ecotroph) referenced to 1950	1.6	-
(*62*)	Fish and other predators (1g to 10^5g)	Global size-structured food web model	2.8	3.2 (*Note 1*)
(*20*)	All marine animals (10^{-5}g to 10^8g)	Global individual-based model (Madingley Model), between 65ºS and 65ºN	57 (*Note 2*)	20.1 (*Notes 1,3*)

(*43*)	Mesopelagic fish (trophic level between 3 and 3.5)	Global energy transfer model (Ecotroph), between 40ºS and 40ºN	12.2 *(Note 4)*	-
(*19*)	All marine animals (10^{-5}g to 10^{6}g)	global size-structured macroecological model	14	5.5 (*Note 1*)
(*19*)	All marine animals (1g to 10^{6}g)	global size-structured macroecological model	4.9	4.9 (*Note 1*)
(*59*)	All targeted marine species	Analysis of stock assessment data	0.84	-
(*21*)	All marine animals (multicellular only)	Meta-analysis of published values	13.3 (*Note 5*)	
(*21*)	All marine fish	Meta-analysis of published values	4.7 (*Note 5*)	4.7 (*Note 6*)
(*63*)	Mesopelagic fish	Extrapolation of acoustic data	4.6	-
(*42*)	Mesopelagic fish	Food web model	2.4	-
(*21*)	Humans	Direct calculation	0.4 *(Note 7)*	-
(*53*)	Phytoplankton	Satellite-based estimate	10 *(Note 8)*	-
This study	All commercial marine animals (10g to 10^{5}g)	global size-structured ecological-economic model	3.3	5.0
This study	All marine animals (10g to 10^{5}g)	global size-structured ecological-economic model	6.9 *(Note 9)*	10.5 *(Note 9)*

Notes: (1) Obtained by rescaling the values in column 1, and assuming a size spectrum following a power-law distribution with a slope of -1.05, based on (Boudreau and Dickie 1992), see details in Supplementary Information Section 1. (2) Estimated by spatial integration of the global average biomass density ($1.67 \cdot 10^{5}$ kg km^{-2}) reported in the paper, assuming an area for the ocean between 65ºS and 65ºN of $3.4 \cdot 10^{14}$ m^{2}. (3) Rescaled to a global area of $3.6 \cdot 10^{14}$ m^{2}. (4) Based on Table 1 of the referenced paper, central value assuming trophic efficiency of 10%, and 80% of primary production entering the food chain. (5) Using a conversion between g C to g wet biomass of 6.67, as in the original publication. (6) Obtained assuming that all fish in the referred paper span the biomass range 10g-10^{6}g. (7) Assuming 50kg/human, and a population of 7.8 billions as of 2020. (8) Using a conversion factor of 10g biomass : g C (9) Values for all marine animals (commercial and non-commercial) calculated from a version of the optimized ensemble where 100% of the net primary production is available to the fish size spectra.

Supplementary Table S2. List of model terms.

Symbol	Name	Units
$f_k(m,t)$	Fish biomass spectrum	gwB m^{-2} g^{-1}
$\gamma_k(m,t)$	Individual fish growth rate	g s^{-1}
$\Lambda_k(m)$	Natural mortality rate	s^{-1}
$q_k(t)$	Catchability parameter	m^2 W^{-1} s^{-1}
$\sigma_k(m)$	Selectivity function	non-dimensional
$E_k(t)$	Fishing effort	W m^{-2}
κ_e	Fleet dynamics parameter	W $\$^{-1}$ s^{-1}
$p_k(m)$	Ex-vessel price	$\$\ \mathrm{gwB}^{-1}$
$c_k(t)$	Cost per unit effort	$\$$ W^{-1} s^{-1}
$s_k(m)$	Fraction of energy to reproduction	non-dimensional
$\phi_{\pi,k}$	Fraction of primary production available to fish	non-dimensional
$\pi(m,t)$	Fish production spectrum	gwB m^{-2} s^{-1} g^{-1}
$R_{P,k}(m_0,t)$	Recruitment determined from primary-production	gwB m^{-2} s^{-1}
$R_{e,k}(m_0,t)$	Recruitment determined from egg production and survival	gwB m^{-2} s^{-1}

Supplementary Table S3. List of model parameters used for the large and optimized ensembles, with the associated statistics (mean±SD).

Parameter	Symbol	units	Large ensemble mean and SD	Optimized ensemble mean and SD	References
Activation energy for growth	$\omega_{a,A}$	eV	0.44±0.09	0.41±0.08	(1)
Activation energy for mortality	$\omega_{a,\lambda}$	eV	0.45±0.09	0.47±0.08	(1)
Allometric scaling exponent	b	non-dimensional	0.70±0.05	0.65±0.03	(2)
Allometric growth constant	A_0	$g^{1-b}\ s^{-1}$	4.47±0.50	4.42±0.48	(3)
Trophic efficiency	α	non-dimensional	0.13±0.04	0.15±0.03	(4)
predator-prey mass ratio	β	non-dimensional	4491±2507	5484±2347	(4)
Eppley constant	κ_e	$°C^{-1}$	0.06±0.01	0.06±0.01	(5)
Nutrient concentration	Π^*	mmol C $m^{-3}\ d^{-1}$	0.37±0.10	0.35±0.09	(6)
Mortality constant	ς_1	non-dimensional	0.55±0.57	0.01±0.40	(7)
Allometric mortality scaling	h	non-dimensional	0.54±0.09	0.49±0.08	(7)
Egg survival fraction	s_e	non-dimensional	0.03±0.01	0.02±0.01	(8)
Selectivity position scaling	e_{mT}	non-dimensional	1.00±0.29	0.88±0.29	(9)
Selectivity slope	c_σ	non-dimensional	18.0±3.47	17.8±3.46	(9)

References: (1) (*92*); (2) (*64*, *92*, *93*); (3)(*93*); (4) (*18*, *43*, *94*); (5)(*95*); (6)(*48*); (7)(*74*); (8)(*96–98*)(Dahlberg 1979, Andersen and Pedersen 2009, Pulkkinen, Mäntyniemi et al. 2013); (9)(*34*).

Supplementary Table S4: List of LMEs for the catch to biomass (C:B) ratio analysis from the RAM stock assessment database (*28*). The number of stocks per LME corresponds to the stocks with a spatial distribution that falls by 99% within the boundaries of each specific LME. For each LME, we calculated the total C:B ratio from the summed catch and summed biomass, and averaged the values for the 5 years corresponding to the peak catch.

LME	Number of stocks	Total LME C:B ratio ($year^{-1}$)	SD ($year^{-1}$)
Agulhas Current	2	0.1244	0.0855
Antarctica	1	0.0282	-
Baltic Sea	4	0.1580	0.1982
Benguela Current	4	0.0518	0.0352
Black Sea	7	0.0863	0.1351
California Current	31	0.0861	0.0815
Canary Current	3	0.2041	0.2481
Celtic-Biscay Shelf	11	0.2342	0.1115
East Bering Sea	6	0.0875	0.1184
East China Sea	2	0.3744	0.0892
Gulf of Alaska	38	0.1680	0.1079
Gulf of Mexico	13	0.3949	0.2518
Humboldt Current	2	0.6833	0.3503
Kuroshio Current	4	0.3678	0.0628
Labrador - Newfoundland	16	0.3100	0.5632
Mediterranean Sea	58	0.0953	0.3916
New Zealand Shelf	43	0.0459	0.3970
North Sea	8	0.2902	0.1700
Northeast U.S. Continent Shelf	27	0.2208	0.2638
Patagonian Shelf	2	0.1057	0.3959
Scotian Shelf	2	0.1566	0.0141
Sea of Japan	2	0.8184	0.2573
Sea of Okhotsk	1	0.0629	-
South West Australian Shelf	3	0.0367	0.0220
Southeast Australian Shelf	2	0.3694	0.1983

Supplementary Table S5. Amplification of fish-mediated particle export fluxes with depth (ζ_f), relative to a reference euphotic zone depth of 74m, for different values of the particle flux attenuation coefficients b_p and b_f.

Depth (z, meters)	Export amplification factor ζ_f		
	"Typical" case b_p=0.7, b_f=0.07	"Weak" case b_p=0.6, b_f=0.06	"Strong" case b_p=0.8, b_f=0
100	1.2	1.2	1.3
200	1.9	1.7	2.2
500	3.3	2.8	4.6
1000	5.1	4.1	7.9
2000	7.9	5.9	13.8
4000	14.1	8.6	24.1

Supplementary Table S6. List of assumptions and limitations that contribute to uncertainty in the estimate of global fish biomass, biogeochemical cycling rate, and impact on ocean biogeochemistry discussed in this study. The list is not exhaustive, and its purpose is to highlight potential theoretical, observational, and model elements that require additional research and improvement.

Factor considered	Examples and effects
Observations and model calibration	
Uncertainties in catch data	Catch data are reconstructed from limited and uncertain landing data, and include data-poor regions and fisheries. Different methods are applied to "fill in" the gaps in landing data (*32*, *99*).
Uncertainties in stock assessments	Not all stocks are assessed. Biases exists towards data rich (e.g., European and North American) fisheries . Stock assessments are inherently uncertainty, depending on statistical models constrained by in-situ observations.
Aggregation level of observations	Catch and stock assessment have been aggregated at the level of LMEs for model evaluation. This overlooks local heterogeneity within individual LMEs. Variations at scales smaller than LMEs are not considered by this approach.
Limited model predictive power	The model only explains a fraction of observed variability in fish catches, and catch to biomass ratios by LMEs (Supplementary Figure S2), although to a degree very similar to other marine ecosystem models, e.g. (*37*).
Ecosystem model formulation	
Structural model uncertainty	The model is size-based, but other approaches have been developed, e.g. trait-based, species-based, etc. Many aspects of fish and food web dynamics are highly parameterized (see below). See ref. (*26*) for a list of different approaches to marine ecosystem modeling.
Coarse model resolution	The model runs on a 100km x 100km grid, with day timestep. The model poorly resolve fine scale features such as narrow shelves, islands, coastal upwelling systems, etc. Likewise, temporal variations less than 1 day (e.g., day-night cycles) are not represented, but they may be relevant to feeding and diel vertical migrations.
Simplified 2D dynamics	The model represents vertically integrated fish dynamics and is thus two-dimensional, lumping together pelagic and demersal species. There is no representation of water column variations, or characteristics of benthic habitat.
Marine consumer diversity	The model is parameterized using general characteristics of fish. It implicitly assumes that invertebrates of similar size (e.g. cephalopods, crustaceans) follow similar dynamics, e.g. growth and mortality rates. Vertebrates, in particular marine homeotherm (mammals and birds), are not represented.
Fish diversity	The model represents fish diversity as three groups with different asymptotic size (small, medium, and large fish). Other axes of fish diversity or "traits" are not included, e.g., functional, community, habitat, taxonomic diversity, etc.
Fish size range	The model explicitly represents the range of fish between 10g to 100kg size. Extrapolation to larger sizes is conducted by applying size spectrum theory.
Targeted vs. non-targeted species	The model represents fish targeted by fisheries, because they can be directly constrained by catch and stock assessment data. Extrapolation to non-targeted species is performed based on the total amount of energy available from NPP, and assuming similar dynamics.
Fish life history	The model represents growth from the stage of recruit to the adult stage, using the same dynamics. Thus, it overlooks egg and larval stages, ontogenetic changes in dynamics, feeding strategies, habitat etc.
Explicit movement	There is no transport of biomass between grid cells, as caused by ocean currents, fish swimming, and long-range migrations. The coarse resolution of the model (100km x 100km) likely reduces the impact of missing movement.

Food web dynamics	Energy transfer is implicit in the model, and does not attempt to resolve specific predator-prey interactions. Transfer of energy is parameterized following macroecological principles (*64*). Energy transfer is only a function of NPP, T and trophic level, follows the same dynamics globally, and does not change in response to biomass depletion.
Fishing effort formulation	
Effort dynamics	The model represents a single fishing effort per fish group. Each effort uses a size-dependent gear selectivity with sigmoidal shape. A globally constant catchability is used to determine catch from effort and selectable biomass.
Fisheries economics	A globally constant and uniform cost per unit effort is used. A constant price is used for all fish sizes and groups.
Management	Model effort follows an open access dynamic, and does not account for management and regulation. Note, however that the model is calibrated with observations from the 1990s, when management was limited.
Model forcing uncertainties	
Physical and biogeochemical forcings	The model is forced with climatological T and NPP reconstructions, representative of the recent observational period (late 20th to early 21st century). Interannual variability is ignored, and conditions both for the modern and preindustrial periods are approximated by climatological present-day conditions.
Fishing effort scenarios	The model's fishing effort is forced by a continuous, exponential increase in catchability (representing technological progress). Spatial and species-dependent variations in catchability, price or cost are not included. Note that price and cost are likely minor drivers over the period considered (*23*).
Pollution, eutrophication, habitat degradation	The model assumes the environment was static, and does not explicitly represent anthropogenic impacts other than fisheries, e.g., pollution, eutrophication and habitat degradation, and their changes over time. These effects likely altered biomass, distribution, and diversity of fish over time.
Early fisheries and defaunation	The model explicitly represents commercial fisheries. Early (prehistoric to preindustrial) fisheries and species declines are not explicitly represented. These include early loss of anadromous species, preindustrial subsistence and artisanal fisheries. The impacts of early fisheries and defaunation on the food web are not represented (e.g., removal of marine mammals and anadromous species).
Anthropogenic climate change	The model as used here does not explicitly represent the effects of climate change, although this has been done elsewhere (*23*, *26*). Model forcings are based on NPP and T from the recent observational period, thus they implicitly include current climate conditions. The historical evolution of this change, and climate change-related stressors (physical and biogeochemical) are not included.
Biogeochemical processes	
Mass conservation	The model parameterizes growth (a function of NPP, T and trophic level); other biomass processing rates (respiration, fecal pellet production) are estimated from growth and trophic efficiency. Because only the commercial portion of the ecosystem is resolved, mass conservation is only approximate.
Fecal pellet production	The model parameterizes fecal pellet production as a constant fraction of biomass processed. However, fecal pellet production varies as a function of taxonomy, feeding rate, physiological state, environmental variables, etc. Fecal pellet properties (e.g., size, density, sinking speed) also depend on fish size, taxonomy, etc.
Fish movement and 3D habitat	The model does not represent fish movement and 3D habitat. Movement would impact biogeochemistry via horizontal and vertical migrations (*9*). 3D habitat would impact the location of biogeochemical impacts (e.g., pelagic vs. mid-water vs. benthic fish).

Fish-biogeochemistry coupling	The model does not resolve feedbacks between fisheries and lower trophic levels. E.g. trophic cascades in response to biomass depletion and their impacts on zooplankton, phytoplankton, and nutrients (*100*). These impacts would in turn affect NPP, particle production, and remineralization (*15*).
Earth system coupling	The model represents fish dynamics and biogeochemical impacts as separate components of the Earth System. However, multiple interactions and feedbacks exists between physical, chemical, and biological Earth System components.

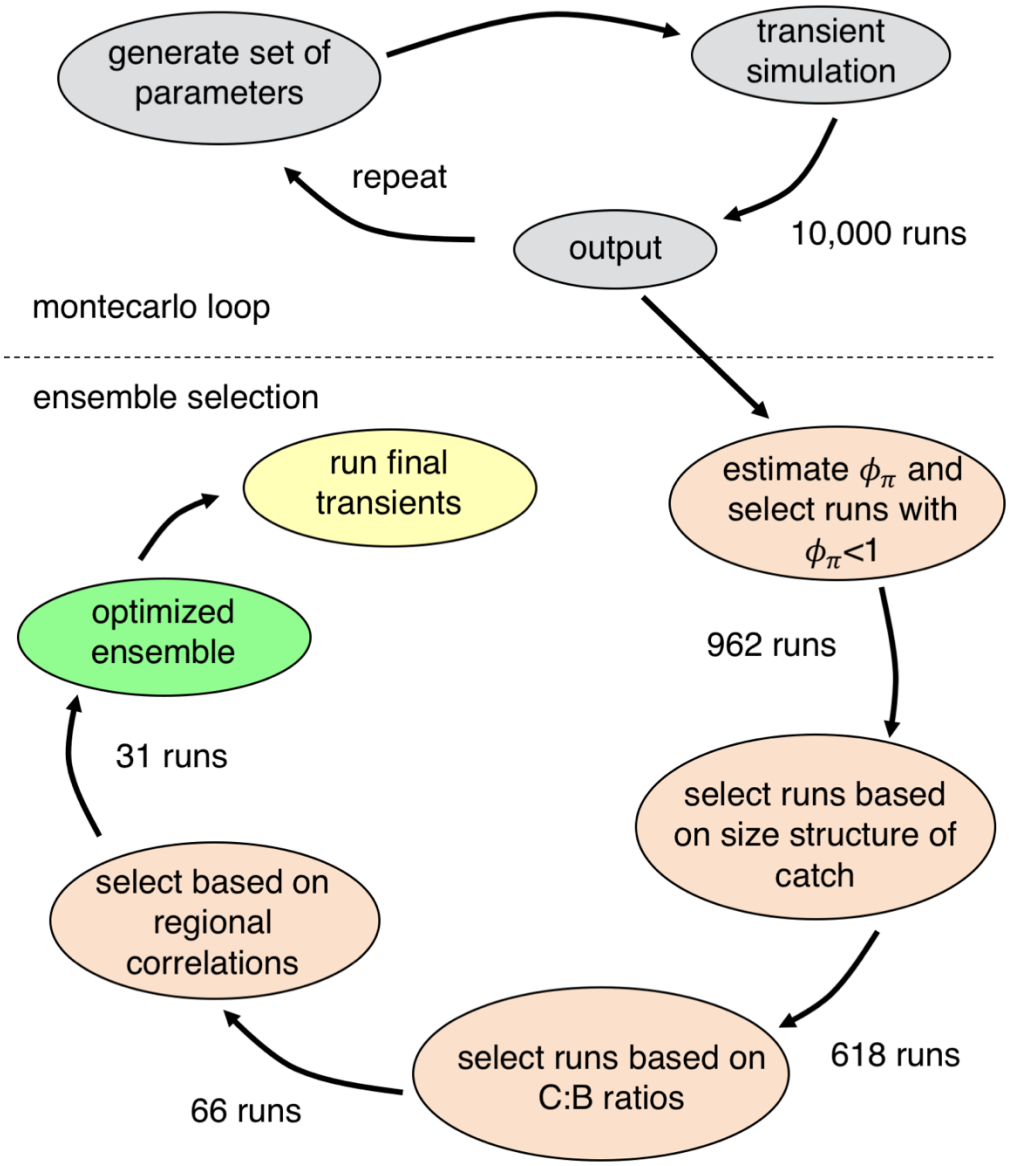

Supplementary Figure S1. Schematic of the steps for the selection of the optimized ensemble model runs. The different steps of the procedure are shown in the colored bubbles. The number of runs remaining after each selection step are shown next to each arrow.

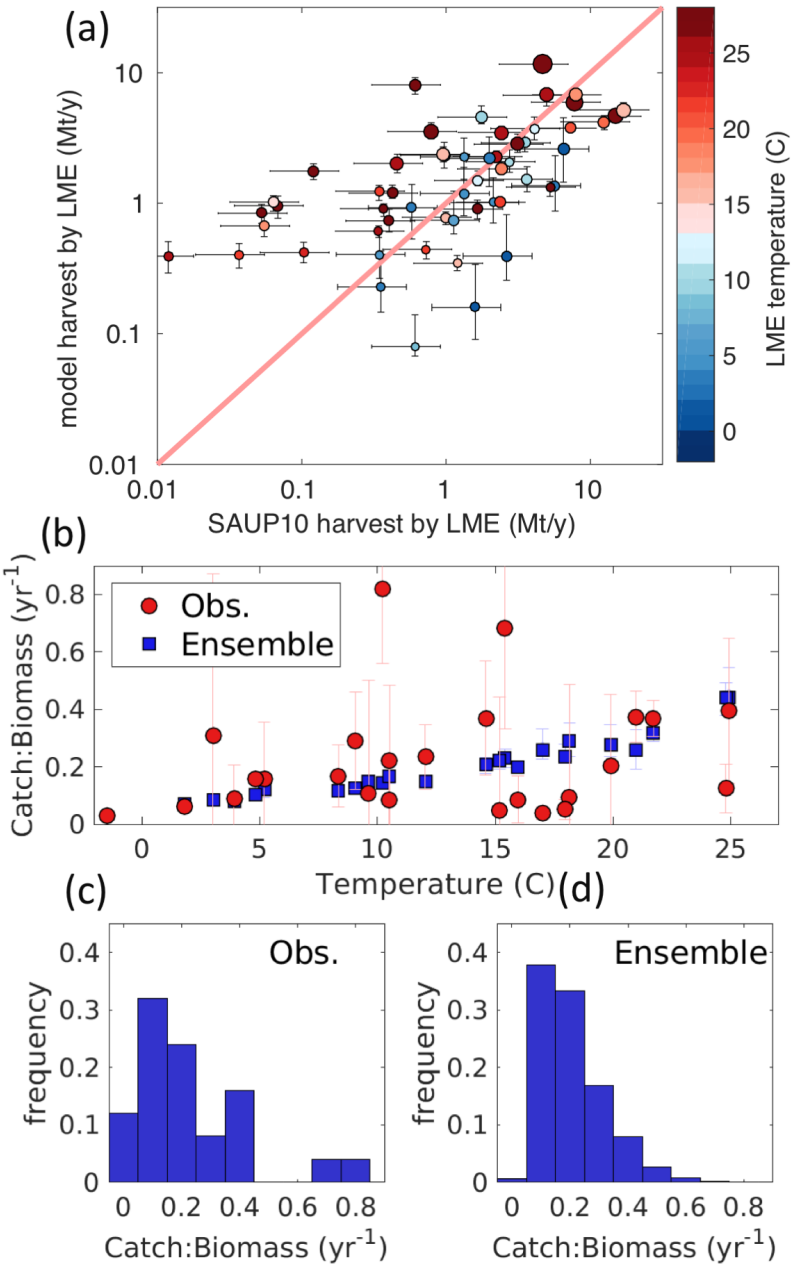

Supplementary Figure S2. Observational and model estimates of catch and catch to biomass (C:B) ratios. **(a)** Model ensemble catches vs estimates from the SAUP database (Mt y^{-1}). Uncertainty on the SAUP catches encompasses a 50% uncertainty range on the estimates, based on the global peak catch uncertainty from ref. (*32*). Uncertainty on the model catches encompasses 90% of the runs (5% to 95% percentiles). The red line is the one-to-one line. Mean temperatures (°C) averaged across LMEs are shown in colors. The area of each dot is proportional to the primary productivity integrated across the corresponding LME. **(b)** C:B ratios

from stock assessments (red dots) and from the model ensemble (blue squares, with 90% confidence range shown as vertical lines), calculated over 24 LMEs, plotted against averaged surface (0-100m) LMEs temperature. **(c)** Probability distribution of C:B ratios from stock assessments, calculated over LMEs. **(d)** As in (c) but for all members of the optimized model ensemble.

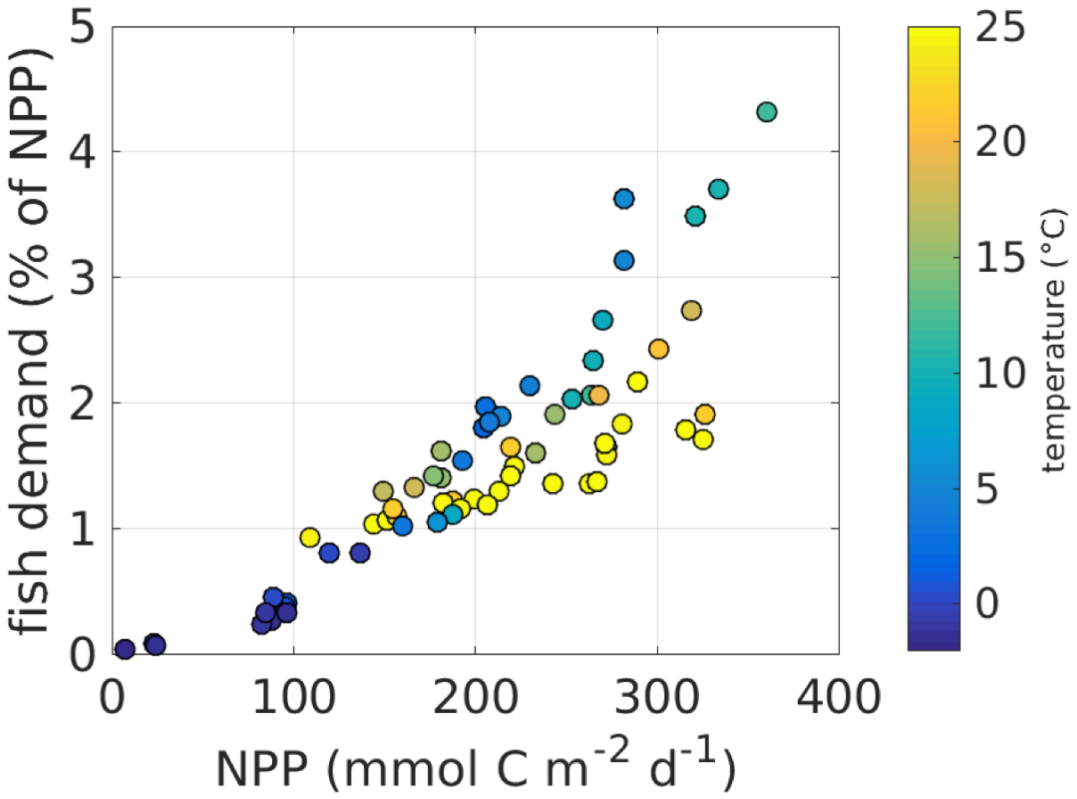

Supplementary Figure S3. Fraction of biomass cycling rate of commercial fish relative to net primary production, versus net primary production. Each dot shows the average over an individual LME region. Colors show average LME temperatures. Model values are means from the optimized ensemble of simulations.

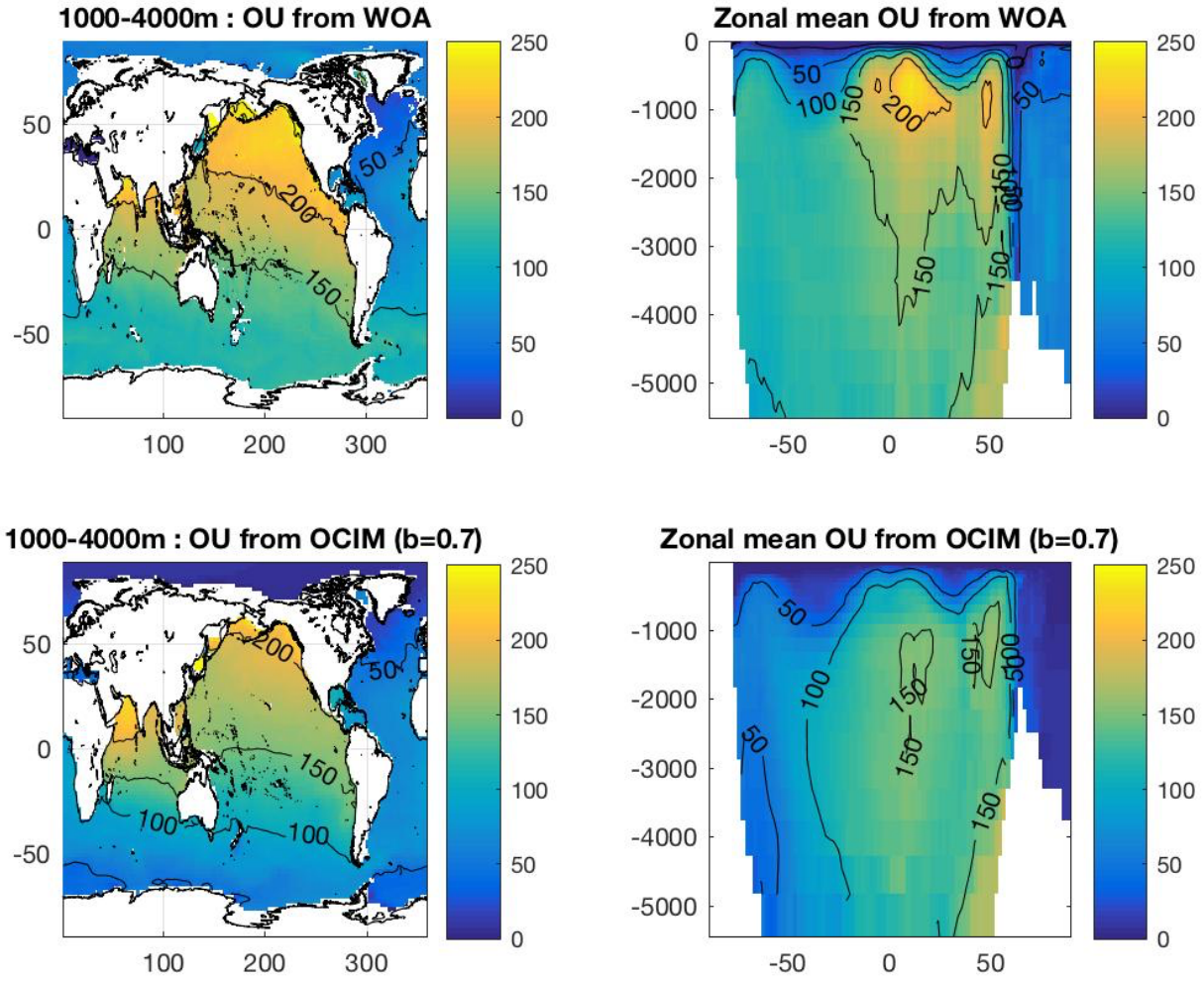

Supplementary Figure S4. Ocean oxygen utilization (OU, in $\mathrm{mmol\,m^{-3}}$) estimated from observations (upper two panels), and from the remineralization of all particles in the ocean inverse circulation model (lower panels). The left panels show the average for the 1000m-4000m depth layer, and the right panels a zonal mean.

REFERENCES AND NOTES

1. C. Le Quere, S. P. Harrison, I. Colin Prentice, E. T. Buitenhuis, O. Aumont, L. Bopp, H. Claustre, L. Cotrim Da Cunha, R. Geider, X. Giraud, Ecosystem dynamics based on plankton functional types for global ocean biogeochemistry models. *Glob. Chang. Biol.* **11**, 2016–2040 (2005).

2. S. Schmidtko, L. Stramma, M. Visbeck, Decline in global oceanic oxygen content during the past five decades. *Nature* **542**, 335–339 (2017).

3. L. Bopp, L. Resplandy, J. C. Orr, S. C. Doney, J. P. Dunne, M. Gehlen, P. Halloran, C. Heinze, T. Ilyina, R. Séférian, J. Tjiputra, M. Vichi, Multiple stressors of ocean ecosystems in the 21st century: Projections with CMIP5 models. *Biogeosciences* **10**, 6225–6245 (2013).

4. J. B. C. Jackson, M. X. Kirby, W. H. Berger, K. A. Bjorndal, L. W. Botsford, B. J. Bourque, R. H. Bradbury, R. Cooke, J. Erlandson, J. A. Estes, Historical overfishing and the recent collapse of coastal ecosystems. *Science* **293**, 629–637 (2001).

5. J. A. Estes, J. Terborgh, J. S. Brashares, M. E. Power, J. Berger, W. J. Bond, S. R. Carpenter, T. E. Essington, R. D. Holt, J. B. C. Jackson, R. J. Marquis, L. Oksanen, T. Oksanen, R. T. Paine, E. K. Pikitch, W. J. Ripple, S. A. Sandin, M. Scheffer, T. W. Schoener, J. B. Shurin, A. R. E. Sinclair, M. E. Soulé, R. Virtanen, D. A. Wardle, Trophic downgrading of planet earth. *Science* **333**, 301–306 (2011).

6. R. T. Paine, Food webs: Linkage, interaction strength and community infrastructure. *J. Anim. Ecol.* **49**, 666 (1980).

7. J. K. Baum, B. Worm, Cascading top-down effects of changing oceanic predator abundances. *J. Anim. Ecol.* **78**, 699–714 (2009).

8. M. J. Vanni, Nutrient cycling by animals in freshwater ecosystems. *Annu. Rev. Ecol. Syst.* **33**, 341–370 (2002).

9. C. E. Doughty, J. Roman, S. Faurby, A. Wolf, A. Haque, E. S. Bakker, Y. Malhi, J. B. Dunning, J.-C. Svenning, Global nutrient transport in a world of giants. *Proc. Natl. Acad. Sci. U.S.A.* **113**, 868–

873 (2015).

10. J. E. Allgeier, D. E. Burkepile, C. A. Layman, Animal pee in the sea: Consumer-mediated nutrient dynamics in the world's changing oceans. *Glob. Chang. Biol.* **23**, 2166–2178 (2017).

11. G. K. Saba, D. K. Steinberg, Abundance, composition, and sinking rates of fish fecal pellets in the Santa Barbara Channel. *Sci. Rep.* **2**, 716 (2012).

12. P. C. Davison, D. M. Checkley Jr, J. A. Koslow, J. Barlow, Carbon export mediated by mesopelagic fishes in the northeast Pacific Ocean. *Prog. Oceanogr.* **116**, 14–30 (2013).

13. D. Bianchi, E. D. Galbraith, D. A. Carozza, K. A. S. Mislan, C. A. Stock, Intensification of open-ocean oxygen depletion by vertically migrating animals. *Nat. Geosci.* **6**, 545–548 (2013).

14. R. W. Wilson, F. J. Millero, J. R. Taylor, P. J. Walsh, V. Christensen, S. Jennings, M. Grosell, Contribution of fish to the marine inorganic carbon cycle. *Science* **323**, 359–362 (2009).

15. J. Getzlaff, A. Oschlies, Pilot study on potential impacts of fisheries-induced changes in zooplankton mortality on marine biogeochemistry. *Global Biogeochem. Cycles* **31**, 1656–1673 (2017).

16. O. Aumont, O. Maury, S. Lefort, L. Bopp, Evaluating the potential impacts of the diurnal vertical migration by marine organisms on marine biogeochemistry. *Global Biogeochem. Cycles* **32**, 1622–1643 (2018).

17. G. K. Saba, A. B. Burd, J. P. Dunne, S. Hernández-León, A. H. Martin, K. A. Rose, J. Salisbury, D. K. Steinberg, C. N. Trueman, R. W. Wilson, Toward a better understanding of fish-based contribution to ocean carbon flux. *Limnol. Oceanogr.* **66**, 1639–1664 (2021).

18. S. Jennings, F. Melin, J. L. Blanchard, R. M. Forster, N. K. Dulvy, R. W. Wilson, Global-scale predictions of community and ecosystem properties from simple ecological theory. *Proc. R. Soc. B Biol. Sci.* **275**, 1375–1383 (2008).

19. S. Jennings, K. Collingridge, Predicting consumer biomass, size-structure, production, catch potential, responses to fishing and associated uncertainties in the world's marine ecosystems. *PLOS*

ONE **10**, e0133794 (2015).

20. M. B. J. Harfoot, T. Newbold, D. P. Tittensor, S. Emmott, J. Hutton, V. Lyutsarev, M. J. Smith, J. P. W. Scharlemann, D. W. Purves, Emergent global patterns of ecosystem structure and function from a mechanistic general ecosystem model. *PLOS Biol.* **12**, e1001841 (2014).

21. Y. M. Bar-On, R. Phillips, R. Milo, The biomass distribution on Earth. *Proc. Natl. Acad. Sci. U.S.A.* **115**, 6506–6511 (2018).

22. R. A. Myers, B. Worm, Rapid worldwide depletion of predatory fish communities. *Nature* **423**, 280–283 (2003).

23. E. D. Galbraith, D. A. Carozza, D. Bianchi, A coupled human-Earth model perspective on long-term trends in the global marine fishery. *Nat. Commun.* **8**, 14884 (2017).

24. H. K. Lotze, B. Worm, Historical baselines for large marine animals. *Trends Ecol. Evol.* **24**, 254–262 (2009).

25. C. M. Free, J. T. Thorson, M. L. Pinsky, K. L. Oken, J. Wiedenmann, O. P. Jensen, Impacts of historical warming on marine fisheries production. *Science* **363**, 979–983 (2019).

26. H. K. Lotze, D. P. Tittensor, A. Bryndum-Buchholz, T. D. Eddy, W. W. L. Cheung, E. D. Galbraith, M. Barange, N. Barrier, D. Bianchi, J. L. Blanchard, L. Bopp, M. Büchner, C. M. Bulman, D. A. Carozza, V. Christensen, M. Coll, J. P. Dunne, E. A. Fulton, S. Jennings, M. C. Jones, S. Mackinson, O. Maury, S. Niiranen, R. Oliveros-Ramos, T. Roy, J. A. Fernandes, J. Schewe, Y. J. Shin, T. A. M. Silva, J. Steenbeek, C. A. Stock, P. Verley, J. Volkholz, N. D. Walker, B. Worm, Global ensemble projections reveal trophic amplification of ocean biomass declines with climate change. *Proc. Natl. Acad. Sci. U.S.A.* **116**, 12907–12912 (2019).

27. G. Mariani, W. W. L. Cheung, A. Lyet, E. Sala, J. Mayorga, L. Velez, S. D. Gaines, T. Dejean, M. Troussellier, D. Mouillot, Let more big fish sink: Fisheries prevent blue carbon sequestration—Half in unprofitable areas. *Sci. Adv.* **6**, eabb4848 (2020).

28. D. Ricard, C. Minto, O. P. Jensen, J. K. Baum, Examining the knowledge base and status of

commercially exploited marine species with the RAM legacy stock assessment database. *Fish.* **13**, 380–398 (2011).

29. L. Kavanagh, E. Galbraith, Links between fish abundance and ocean biogeochemistry as recorded in marine sediments. *PLOS ONE* **13**, e0199420 (2018).

30. S. Jennings, J. L. Blanchard, Fish abundance with no fishing: Predictions based on macroecological theory. *J. Anim. Ecol.* **73**, 632–642 (2004).

31. V. Christensen, M. Coll, J. Buszowski, W. W. L. Cheung, T. Frölicher, J. Steenbeek, C. A. Stock, R. A. Watson, C. J. Walters, The global ocean is an ecosystem: Simulating marine life and fisheries. *Glob. Ecol. Biogeogr.* **24**, 507–517 (2015).

32. D. Pauly, D. Zeller, Catch reconstructions reveal that global marine fisheries catches are higher than reported and declining. *Nat. Commun.* **7**, 10244 (2016).

33. D. A. Carozza, D. Bianchi, E. D. Galbraith, The ecological module of BOATS-1.0: A bioenergetically constrained model of marine upper trophic levels suitable for studies of fisheries and ocean biogeochemistry. *Geosci. Model Dev.* **9**, 1545–1565 (2016).

34. D. A. Carozza, D. Bianchi, E. D. Galbraith, Formulation, general features and global calibration of a bioenergetically-constrained fishery model. *PLOS ONE* **12**, e0169763 (2017).

35. T. A. Branch, O. P. Jensen, D. Ricard, Y. Ye, R. A. Y. Hilborn, Contrasting global trends in marine fishery status obtained from catches and from stock assessments. *Conserv. Biol.* **25**, 777–786 (2011).

36. D. Pauly, R. Hilborn, T. A. Branch, Fisheries: Does catch reflect abundance? *Nature* **494**, 303–306 (2013).

37. C. A. Stock, J. G. John, R. R. Rykaczewski, R. G. Asch, W. W. L. Cheung, J. P. Dunne, K. D. Friedland, V. W. Y. Lam, J. L. Sarmiento, R. A. Watson, Reconciling fisheries catch and ocean productivity. *Proc. Natl. Acad. Sci. U.S.A.* **114**, E1441–E1449 (2017).

38. J. Guiet, E. D. Galbraith, D. Bianchi, W. W. L. Cheung, Bioenergetic influence on the historical

development and decline of industrial fisheries. *ICES J. Mar. Sci.* **77**, 1854–1863 (2020).

39. V. H. Smith, S. B. Joye, R. W. Howarth, Eutrophication of freshwater and marine ecosystems. *Limnol. Oceanogr.* **51**, 351–355 (2006).

40. D. J. McCauley, M. L. Pinsky, S. R. Palumbi, J. A. Estes, F. H. Joyce, R. R. Warner, Marine defaunation: Animal loss in the global ocean. *Science* **347**, 1255641 (2015).

41. H. Whitehead, Estimates of the current global population size and historical trajectory for sperm whales. *Mar. Ecol. Prog. Ser.* **242**, 295–304 (2002).

42. T. R. Anderson, A. P. Martin, R. S. Lampitt, C. N. Trueman, S. A. Henson, D. J. Mayor, J. Link, Quantifying carbon fluxes from primary production to mesopelagic fish using a simple food web model. *ICES J. Mar. Sci.* **76**, 690–701 (2019).

43. X. Irigoien, T. A. Klevjer, A. Røstad, U. Martinez, G. Boyra, J. L. Acuña, A. Bode, F. Echevarria, J. I. Gonzalez-Gordillo, S. Hernandez-Leon, S. Agusti, D. L. Aksnes, C. M. Duarte, S. Kaartvedt, Large mesopelagic fishes biomass and trophic efficiency in the open ocean. *Nat. Commun.* **5**, 3271 (2014).

44. E. D. Galbraith, P. Le Mézo, G. S. Hernandez, D. Bianchi, D. Kroodsma, Growth limitation of marine fish by low iron availability in the open ocean. *Front. Mar. Sci.* **6** (2019).

45. R. A. Watson, W. W. L. Cheung, J. A. Anticamara, R. U. Sumaila, D. Zeller, D. Pauly, Global marine yield halved as fishing intensity redoubles. *Fish.* **14**, 493–503 (2013).

46. Y. Rousseau, R. A. Watson, J. L. Blanchard, E. A. Fulton, Evolution of global marine fishing fleets and the response of fished resources. *Proc. Natl. Acad. Sci. U.S.A.* **116**, 12238–12243 (2019).

47. J. H. Ryther, Photosynthesis and fish production in the sea. The production of organic matter and its conversion to higher forms of life vary throughout the world ocean. *Science* **166**, 72–76 (1969).

48. J. P. Dunne, R. A. Armstrong, A. Gnanadesikan, J. L. Sarmiento, Empirical and mechanistic models for the particle export ratio. *Global Biogeochem. Cycles.* **19**, (2005).

49. B. Kooijman, *Dynamic Energy Budget Theory for Metabolic Organisation* (Cambridge Univ. Press, ed. 3, 2009).

50. F. Primeau, On the variability of the exponent in the power law depth dependence of POC flux estimated from sediment traps. *Deep. Res. Part I Oceanogr. Res. Pap.* **53**, 1335–1343 (2006).

51. P. W. Boyd, H. Claustre, M. Levy, D. A. Siegel, T. Weber, Multi-faceted particle pumps drive carbon sequestration in the ocean. *Nature* **568**, 327–335 (2019).

52. T. DeVries, The oceanic anthropogenic CO2sink: Storage, air-sea fluxes, and transports over the industrial era. *Global Biogeochem. Cycles* **28**, 631–647 (2014).

53. P. G. Falkowski, R. T. Barber, V. Smetacek, Biogeochemical controls and feedbacks on ocean primary production. *Science* **281**, 200–206 (1998).

54. C. Laufkötter, M. Vogt, N. Gruber, Long-term trends in ocean plankton production and particle export between 1960-2006. *Biogeosciences* **10**, 7373–7393 (2013).

55. L. A. Levin, Manifestation, drivers, and emergence of open ocean deoxygenation. *Annu. Rev. Mar. Sci.* **10**, 229–260 (2018).

56. R. Hilborn, R. O. Amoroso, C. M. Anderson, J. K. Baum, T. A. Branch, C. Costello, C. L. De Moor, A. Faraj, D. Hively, O. P. Jensen, Effective fisheries management instrumental in improving fish stock status. *Proc. Natl. Acad. Sci. U.S.A.* **117**, 2218–2224 (2020).

57. C. M. Duarte, S. Agusti, E. Barbier, G. L. Britten, J. C. Castilla, J.-P. Gattuso, R. W. Fulweiler, T. P. Hughes, N. Knowlton, C. E. Lovelock, Rebuilding marine life. *Nature* **580**, 39–51 (2020).

58. L. A. Anderson, On the hydrogen and oxygen content of marine phytoplankton. *Deep Sea Res. Part I Oceanogr. Res. Pap.* **42**, 1675–1680 (1995).

59. C. Costello, D. Ovando, T. Clavelle, C. Kent Strauss, R. Hilborn, M. C. Melnychuk, T. A. Branch, S. D. Gaines, C. S. Szuwalski, R. B. Cabral, D. N. Rader, A. Leland, Global fishery prospects under contrasting management regimes. *Proc. Natl. Acad. Sci. U.S.A.* **113**, 5125–5129 (2016).

60. V. Christensen, C. J. Walters, R. Ahrens, J. Alder, J. Buszowski, L. B. Christensen, W. W. L. Cheung, J. Dunne, R. Froese, V. Karpouzi, Database-driven models of the world's Large Marine Ecosystems. *Ecol. Model.* **220**, 1984–1996 (2009).

61. L. Tremblay-Boyer, D. Gascuel, R. Watson, V. Christensen, D. Pauly, Modelling the effects of fishing on the biomass of the world's oceans from 1950 to 2006. *Mar. Ecol. Prog. Ser.* **442**, 169–185 (2011).

62. J. R. Watson, C. A. Stock, J. L. Sarmiento, Exploring the role of movement in determining the global distribution of marine biomass using a coupled hydrodynamic—Size-based ecosystem model. *Prog. Oceanogr.* **138**, 521–532 (2014).

63. R. Proud, N. O. Handegard, R. J. Kloser, M. J. Cox, A. S. Brierley, D. Demer, From siphonophores to deep scattering layers: Uncertainty ranges for the estimation of global mesopelagic fish biomass. *ICES J. Mar. Sci.* **76**, 718–733 (2019).

64. J. H. Brown, J. F. Gillooly, A. P. Allen, V. M. Savage, G. B. West, Toward a metabolic theory of ecology. *Ecology* **85**, 1771–1789 (2004).

65. M. Edwards, J. P. W. Robinson, M. J. Plank, J. K. Baum, J. L. Blanchard, Testing and recommending methods for fitting size spectra to data. *Methods Ecol. Evol.* **8**, 57–67 (2017).

66. P. R. Boudreau, L. M. Dickie, Biomass spectra of aquatic ecosystems in relation to fisheries yield. *Can. J. Fish. Aquat. Sci.* **49**, 1528–1538 (1992).

67. R. W. Sheldon, A. Prakash, W. H. Sutcliffe, The size distribution of particles in the ocean. *Limnol. Oceanogr.* **17**, 327–340 (1972).

68. J. F. Gillooly, J. H. Brown, G. B. West, V. M. Savage, E. L. Charnov, Effects of size and temperature on metabolic rate. *Science* **293**, 2248–2251 (2001).

69. S. K. Ernest, B. J. Enquist, J. H. Brown, E. L. Charnov, J. F. Gillooly, V. M. Savage, E. P. White, F. A. Smith, E. A. Hadly, J. P. Haskell, Thermodynamic and metabolic effects on the scaling of production and population energy use. *Ecol. Lett.* **6**, 990–995 (2003).

70. M. Hartvig, K. H. Andersen, J. E. Beyer, Food web framework for size-structured populations. *J. Theor. Biol.* **272**, 113–122 (2011).

71. O. Maury, J.-C. Poggiale, From individuals to populations to communities: A dynamic energy budget model of marine ecosystem size-spectrum including life history diversity. *J. Theor. Biol.* **324**, 52–71 (2013).

72. D. Pauly, The Sea Around Us Project: Documenting and communicating global fisheries impacts on marine ecosystems. *AMBIO J. Hum. Environ.* **36**, 290–295 (2007).

73. L. von Bertalanffy, Problems of organic growth. *Nature* **163**, 156–158 (1949).

74. H. Gislason, N. Daan, J. C. Rice, J. G. Pope, Size, growth, temperature and the natural mortality of marine fish. *Fish Fish.* **11**, 149–158 (2010).

75. E. L. Charnov, H. Gislason, J. G. Pope, Evolutionary assembly rules for fish life histories. *Fish Fish.* **14**, 213–224 (2013).

76. R. J. H. Beverton, S. J. Holt, *On the Dynamics of Exploited Fish Populations* (Springer Science & Business Media, 1957), vol. 11.

77. H. S. Gordon, The economic theory of a common-property resource: The fishery. *J. Polit. Econ.* **62**, 124–142 (1954).

78. M. B. Schaefer, Some aspects of the dynamics of populations important to the management of the commercial marine fisheries. *Inter-American Trop. Tuna Comm. Bull.* **1**, 23–56 (1954).

79. D. Pauly, M. L. D. Palomares, "An empirical equation to predict annual increases in fishing efficiency," Working Paper 2010-07, UBC Fisheries Centre, Vancouver, BC, Canada, 2010.

80. D. Squires, N. Vestergaard, Technical change and the commons. *Rev. Econ. Stat.* **95**, 1769–1787 (2013).

81. O. Maury, B. Faugeras, Y.-J. Shin, J.-C. Poggiale, T. Ben Ari, F. Marsac, Modeling environmental effects on the size-structured energy flow through marine ecosystems. Part 1: The model. *Prog.*

Oceanogr. **74**, 479–499 (2007).

82. S. Jennings, J. K. Pinnegar, N. V. C. Polunin, T. W. Boon, Weak cross-species relationships between body size and trophic level belie powerful size-based trophic structuring in fish communities. *J. Anim. Ecol.* **70**, 934–944 (2001).

83. R. A. Locarnini, A. V Mishonov, J. I. Antonov, T. P. Boyer, H. E. Garcia, *World Ocean Atlas 2005, Vol. 1: Temperature*, S. Levitus, Ed. (U.S. Government Printing Office, 2006).

84. K. H. Andersen, N. S. Jacobsen, K. D. Farnsworth, The theoretical foundations for size spectrum models of fish communities. *Can. J. Fish. Aquat. Sci.* **73**, 575–588 (2015).

85. D. Pauly, V. Christensen, Primary production required to sustain global fisheries. *Nature* **374**, 255–257 (1995).

86. J. H. Martin, G. A. Knauer, D. M. Karl, W. W. Broenkow, VERTEX: Carbon cycling in the northeast Pacific. *Deep Sea Res. Part A Oceanogr. Res. Pap.* **34**, 267–285 (1987).

87. I. Kriest, A. Oschlies, On the treatment of particulate organic matter sinking in large-scale models of marine biogeochemical cycles. *Biogeosciences* **5**, 55–72 (2008).

88. T. DeVries, F. Primeau, Dynamically and observationally constrained estimates of water-mass distributions and ages in the global ocean. *J. Phys. Oceanogr.* **41**, 2381–2401 (2011).

89. O. Duteil, W. Koeve, A. Oschlies, D. Bianchi, E. Galbraith, I. Kriest, R. Matear, A novel estimate of ocean oxygen utilisation points to a reduced rate of respiration in the ocean interior. *Biogeosciences* **10**, 7723–7738 (2013).

90. T. DeVries, T. Weber, The export and fate of organic matter in the ocean: New constraints from combining satellite and oceanographic tracer observations. *Global Biogeochem. Cycles* **31**, 535–555 (2017).

91. T. Weber, J. A. Cram, S. W. Leung, T. DeVries, C. Deutsch, Deep ocean nutrients imply large latitudinal variation in particle transfer efficiency. *Proc. Natl. Acad. Sci. U.S.A.* **113**, 8606–8611

(2016).

92. V. M. Savage, J. F. Gillooly, J. H. Brown, G. B. West, E. L. Charnov, Effects of body size and temperature on population growth. *Am. Nat.* **163**, 429–441 (2004).

93. H. Andersen, J. E. Beyer, Size structure, not metabolic scaling rules, determines fisheries reference points. *Fish Fish.* **16**, 1–22 (2013).

94. C. Barnes, D. Maxwell, D. C. Reuman, S. Jennings, Global patterns in predator-prey size relationships reveal size dependency of trophic transfer efficiency. *Ecology* **91**, 222–232 (2010).

95. E. Bissinger, D. J. S. Montagnes, D. Atkinson, Predicting marine phytoplankton maximum growth rates from temperature: Improving on the Eppley curve using quantile regression. *Limnol. Oceanogr.* **53**, 487–493 (2008).

96. D. Dahlberg, A review of survival rates of fish eggs and larvae in relation to impact assessments. *Mar. Fish. Rev.* **41**, 1–12 (1979).

97. K. H. Andersen, M. Pedersen, Damped trophic cascades driven by fishing in model marine ecosystems. *Proc. R. Soc. B* **277**, 795–802 (2010).

98. H. Pulkkinen, S. Mäntyniemi, Y. Chen, Maximum survival of eggs as the key parameter of stock–recruit meta-analysis: Accounting for parameter and structural uncertainty. *Can. J. Fish. Aquat. Sci.* **70**, 527–533 (2013).

99. R. A. Watson, A database of global marine commercial, small-scale, illegal and unreported fisheries catch 1950–2014. *Sci. Data* **4**, 1–9 (2017).

100. K. T. Frank, B. Petrie, J. S. Choi, W. C. Leggett, Trophic cascades in a formerly cod-dominated ecosystem. *Science* **308**, 1621–1623 (2005).